

# Bench test of TRIP-t

Leo Bellantoni, Paul Rubinov

D0 note #####

**Abstract** A report of the bench tests of the first TRIP-t chip, and a short summary of how the chip should be operated.

Draft

## ***Description of the TRIP-t***

The TRIP-t chip, designed by Abderrezak Mekkaoui, Tom Zimmerman and Jim Hoff is the part of the front end of the D0 electronics for the VLPC based detectors. Its inputs are the analog pulses from the fibers after amplification by the VLPCs and digital timing inputs to control e.g. the time window over which the system should be sensitive to pulses. The outputs of the TRIP-t are (1) a digital signal to use for triggering; (2) an analog pulse ( $\sim 1V$ ) that is proportional to the amplitude of the input from the VLPC, called the *A*-pulse; (3) an analog pulse ( $\sim 1V$ ) that is proportional to the time between the firing of the discriminator and the closing of the time-gate, called the *t*-pulse. The chip contains an analog pipeline just before the final output drivers.

The TRIP-t is a modification of the TRIP chip; see D0 notes 4009 and 4076. Documentation is at  
`smb://D0server6/projects/TriggerElectronics/CAE/Run_I Ib_AFE.`

Figure 1 shows a simplified functional diagram of the TRIP-t. The front end, shown in simplified functional form in Figure 2, produces the three primary outputs of the chip. The *A*-pulse and *t*-pulse outputs are stored in analog pipelines, and the output of these is selected by the SKIPB signal, which is in effect the L1 YES signal. Outputs to form trigger signals are created by discriminators in the front end, and readout quickly through the digital multiplexer. The operation of the front end is controlled by a set of DACs that determine parameters such as the drive currents for opamps. Although it is not shown in Figure 1, the Program Interface also provides some parameters to the pipeline and the final output drivers of the *A*- and *t*-pulses.

## ***Operation of the TRIP-t***

The programming of the DACs for the TRIP-t is basically the same as it was

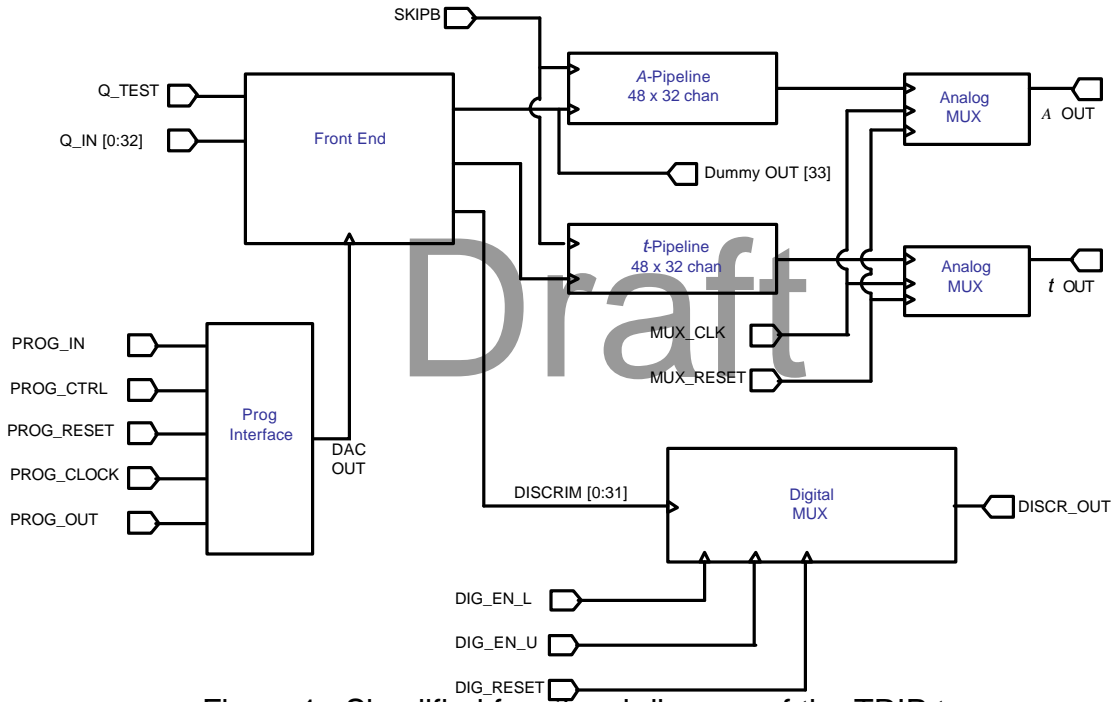


Figure 1. Simplified functional diagram of the TRIP-t

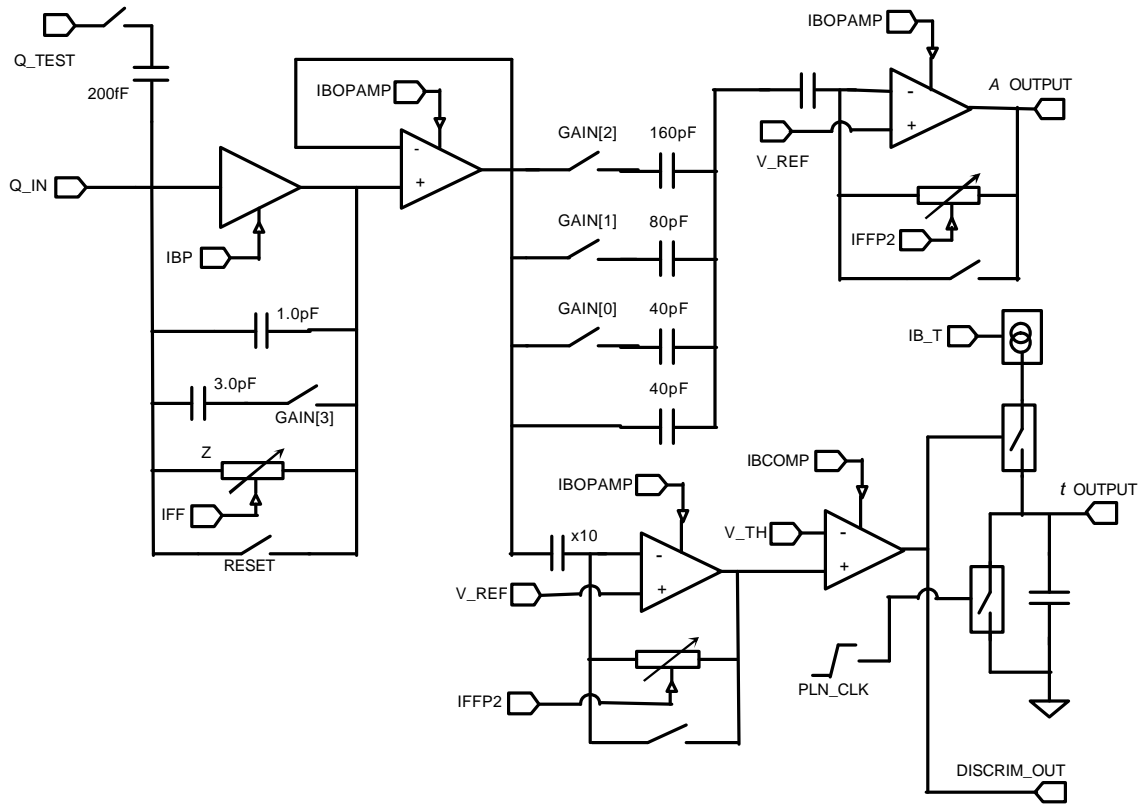


Figure 2. Simplified functional diagram of the TRIP-t front end.

for the TRIP chip, and is described in D0 note 4009. However, the meanings of the registers given in that document have changed. The new definitions and the values used here are given in Table 1. The values used here should be close to those used in the final installation, except for registers 6 and 11.

Register	Name	Default value	Comment
1	IBP	130	Preamp drive current
2	IBBNFoll	120	Preamp feedback control
3	IFF	40	Preamp feedback control
4	IBPIFF1REF	160	Preamp reset strength
5	IBOPAMP	255	Opamp drive current
6	IB_T	80	Time circuit current source
7	IFFP2	42	Opamp feedback control
8	IBCOMP	10	Comparator drive current
9	V_REF	170	Ref voltage for opamps 2 & 3
10	V_TH	243	Ref voltage for comparator
11[5:0]	PIPEDELAY	6	Pipeline depth
11[9:6]	GAIN	0111	Gain; high bit is negative logic
12	IRWSEL	15	Drive currents for pipeline R/W
13	LUCKB	42	Do not use
14	INJECT	none	Which channels to test-pulse

Table 1. Register settings use here. In situ, IB\_T will be near 60 to provide an 80nsec range for the  $t$ -pulse, and PIPEDELAY will be 31.

Correct operation also requires specification of the timing of the signals input to the chip. A spreadsheet showing all the signals is available at `smb://D0server6/projects/TriggerElectronics/CAE/Run_Iib_AFE/Trip-t\ Chip/TRIP-t\ from\ Leo/Review_Apr05/DG2020\ copy.xls`. Figure 3 shows a detail of the critical reset/gating signals.

The PRE\_RST signal is actually three signals; PRE\_RST itself, and two inverted signals, P2A\_RSTB and P2B\_RSTB. All have the same timing; the reset is on for 245ns and then off for 155ns, making a cycle time of 400ns, close to the 393ns beam crossing time. The signals DIGENL, DIGENU, and DIGENB are the signals to output the discriminator signals; the first 16 channels are sent out on DIGENL and the same 16 lines show the second 16 discriminator results on DIGENU. These signals are 20ns wide and their positioning inside the PRE\_RST pulse is not critical. The PLN\_CLK signal determines the gate for which the input is sensitive, unless PR1 was high at an earlier low to high transition of PLN\_CLK. In the latter case, the pipeline is read out. In figure 3, the chip will be sensitive to pulses at the input between  $t = 9420ns$  and  $t=9520ns$ . PRE\_RST

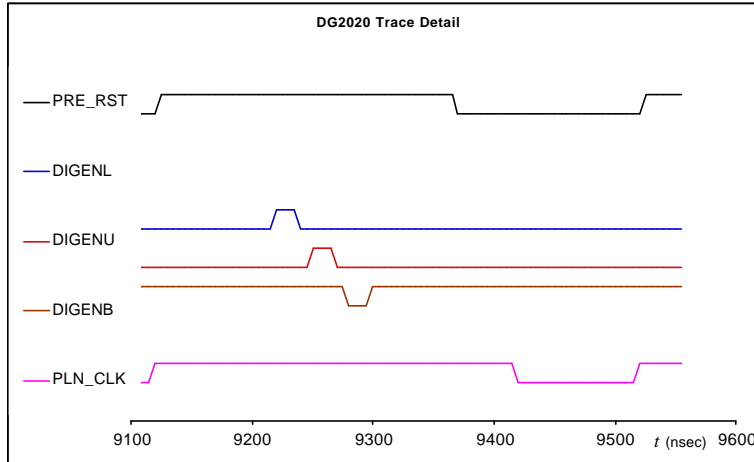


Figure 3. Reset and gating signal details

must finish  $50ns$  before the `PLN_CLK` is active, and there is a  $5ns$  gap after the gate closes before the next `PRE_RST` begins.

### ***Discriminator test results***

The setting of  $R_{10}$  in Table 1 corresponds to a discriminator threshold of  $8fC$ , assuming that the  $200fF$  capacitor on the `Q_TEST` line of Figure 2 is indeed  $200fF$ . Channel to channel variation of the capacitance within a given chip should be quite small – on the order of 5% – but the absolute scale of these capacitances is guaranteed to only the 30% level. Figure 4 shows the discriminator turn-on

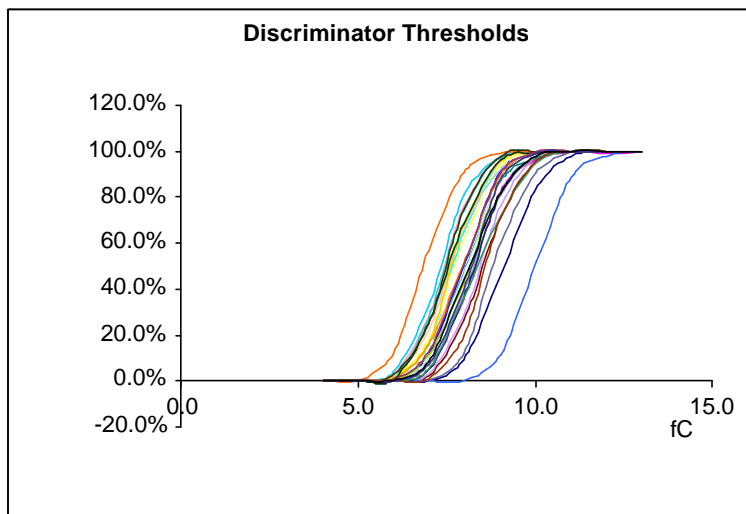


Figure 4. Discriminator threshold curves.

curves for 32 channels. The curves fit a Gaussian distribution well. Figure 5 shows the distributions of the fitted means and widths. Thresholds were measured with realistic capacitances on the outputs.

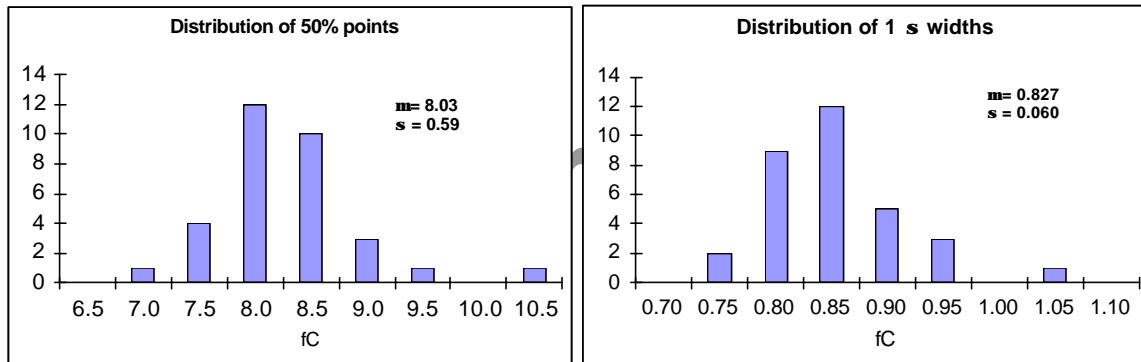


Figure 5. Distributions of fitted means and widths of the discriminator turn-on curves for 32 channels.

### ***A-pulse test results***

There was a design problem with the *A*-pulse outputs, created by the final output drivers at the end of the pipeline. The problem seems easy to remedy.

First we show the distribution of *A*-pulse outputs as a function of time in the window, in Figure 6, for 5 channels. This result is essentially the same as for the TRIP; the rise time is essentially the width of the injected test pulse and the roll-off reflects the bandwidth of the preamp. Generally, *A*-pulse data shown here was taken at  $t = 35ns$  on Figure 6.

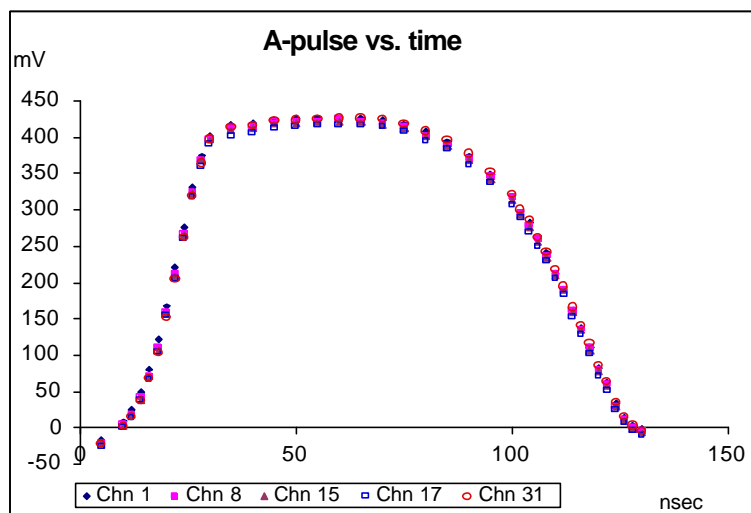


Figure 6. Pulse window for 100ns gate.

Figure 7 shows the  $A$ -pulse output as a function of injected charge for the highest gain setting, which is the gain planned for use in the fiber tracker. Note the nonlinearity at low pulse amplitudes<sup>1</sup>. Figure 8 shows the differential gain, *i.e.*,

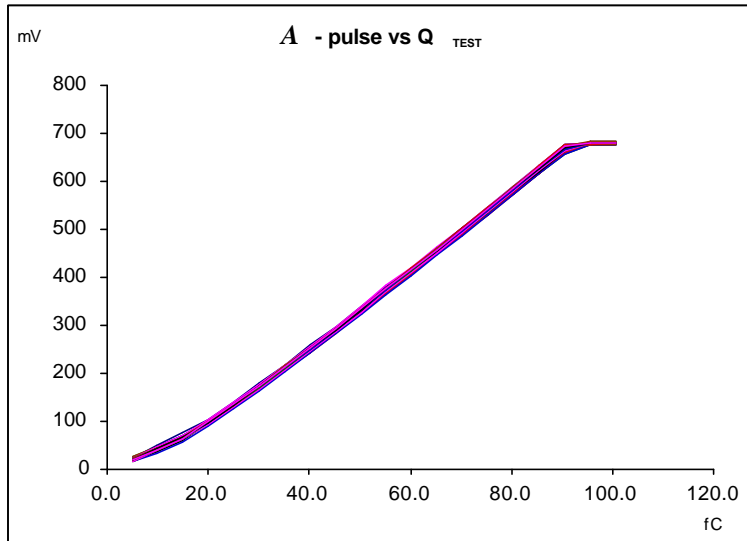


Figure 7. Nonlinearity in  $A$ -pulse outputs.

the derivative of the curves in Figure 7. In the range below 40 fC, the differential gain drops off, finally going down to nearly half the correct value.

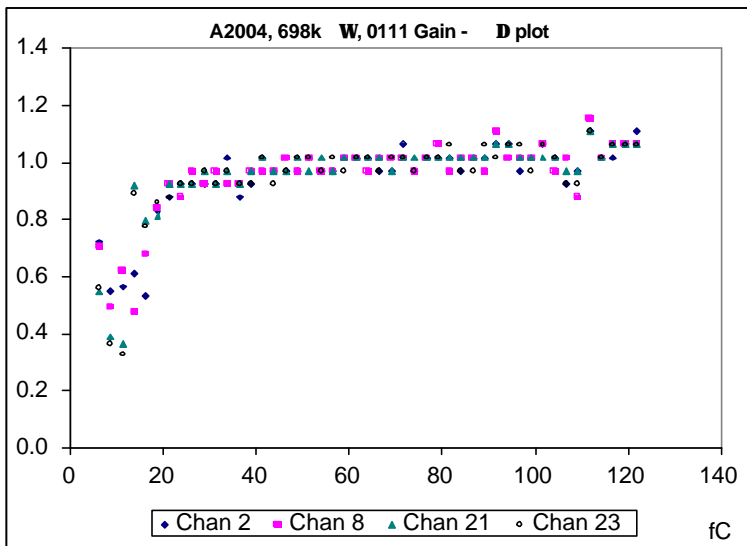


Figure 8. Nonlinearity in  $A$ -pulse differential gain.

<sup>1</sup> Noise levels on the  $A$ -pulse and  $t$ -pulse outputs was Gaussian, with about 3mV RMS under most circumstances. There was no effort at distinguishing true noise in the TRIP- $t$  from noise induced by the test setup.

The nonlinearity is well modeled in SPICE simulation. The left side of Figure 9 shows the simulated version of Figure 8. The curve OUTAP refers to the output of the analog pipeline; OUTAPBUF is the output of the final driver buffer that follows the pipeline. On the right side of Figure 9, the same curve is shown but with  $n$  channel FETs in the output buffer replaced  $p$  channel FETs, as shown in Figure 10.

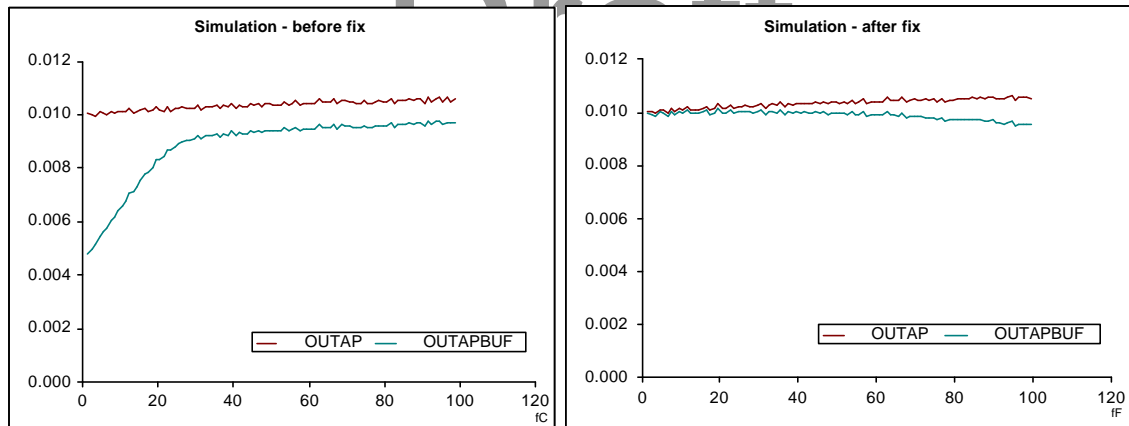


Figure 9. Differential gain in SPICE simulation of pipeline output buffer before and after FET revision. No capacitive load at the output has been allowed for.

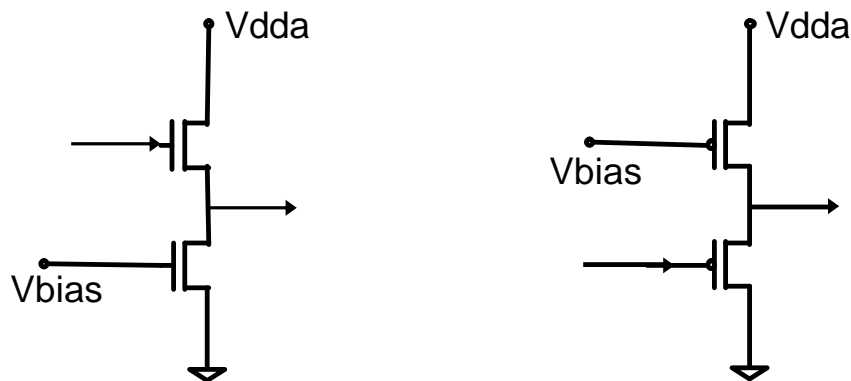


Figure 10.  $n$  channel to  $p$  channel FET substitution in final driver stage.

The performance specification is driven by the fact that output of the TRIP-t will be fed into a 7 bit ADC. Figure 11 shows the residual of a linear fit to the integral of the OUTAPBUF curve from the right side of Figure 9. The maximum residual occurs at full scale and is about  $5mV$ ; 7 bits precision on a  $1V$  signal<sup>2</sup> is  $7.8mV$ .

<sup>2</sup> The running conditions in the SPICE simulation were slightly different than in the test bench runs.

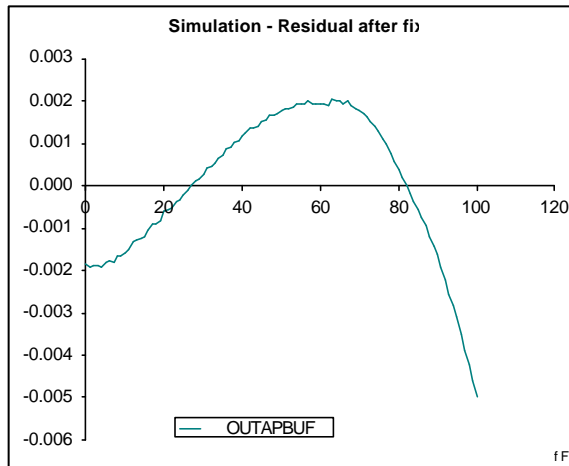


Figure 11. Residual nonlinearity in SPICE simulation after FET revision.

The gains of the 32 channels were determined by a fit of the measured responses in the region 45 to 85 fC. Figure 12 shows the distribution of gains.

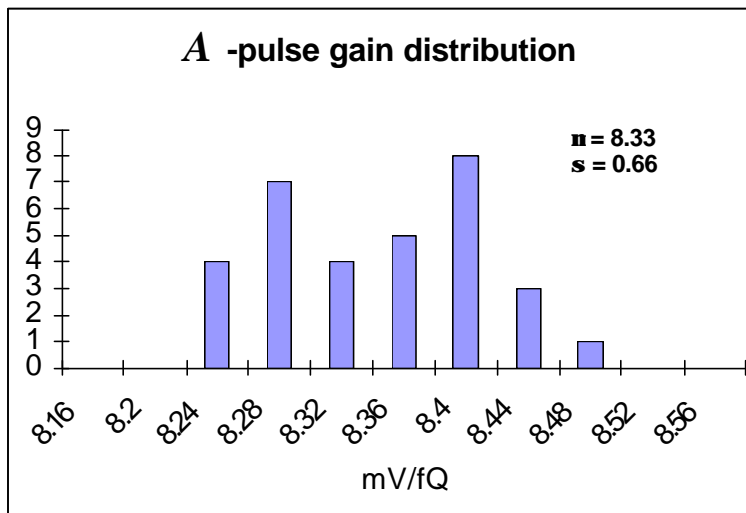


Figure 12. Distribution of measured gains.

### ***t*-pulse test results**

The *t*-pulse output is created by switching the flow of current onto a capacitor at the time when the discriminator fires, and switching the flow off at the close of the gate (*i.e.*, at the low to high transition of PLN\_CLK). The output, taken from this capacitor's charge, consequently becomes lower for later input pulses. Figure 13 shows the *t*-pulse output as a function of injection time for 45fC pulses. Some of the curvature visible at lower output values is undoubtedly due to the output buffer issue, and the correct selection of *t*-pulse gain will need the linearity of the output driver to be corrected.

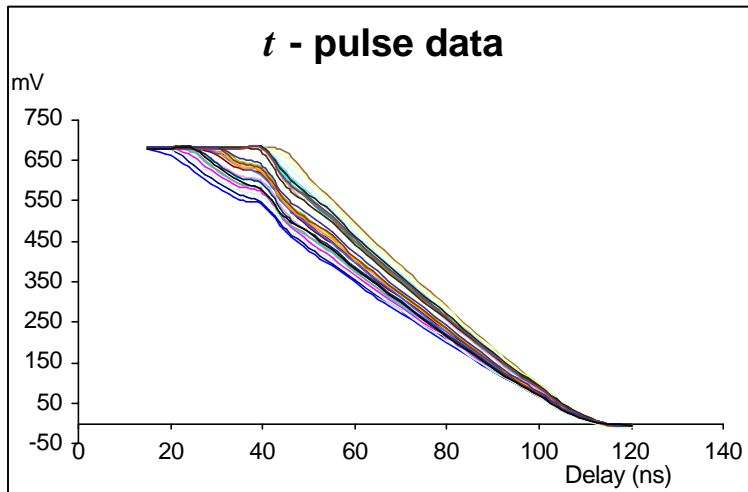


Figure 13. Measured  $t$ -pulse amplitudes as a function of injection time.

Figure 13. Distribution of measured gains for  $t$ -pulse outputs.

Gain variation is relatively larger in the  $t$ -pulse data than in the  $A$ -pulse data; selection of a final operation parameter for  $R_6$  will also require adjustment to the channel of highest  $t$ -pulse gain. Figure 14 shows the distribution of gains after fitting the  $t$ -pulse curves to lines in the regions between 50 and 110 ns

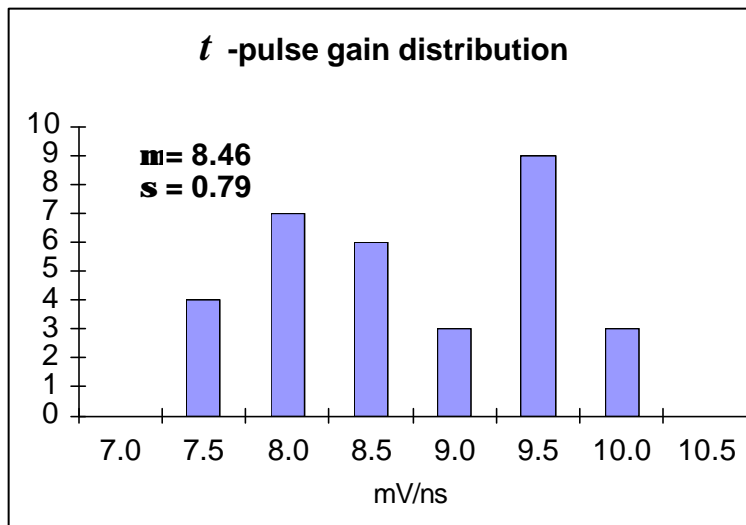


Figure 14. Distribution of gains of  $t$ -pulse outputs.

The residuals of the  $t$ -pulse curves after fitting is shown in Figure 15. The RMS of the residual in this range is 8.3 mV, corresponding to about 1 ns.

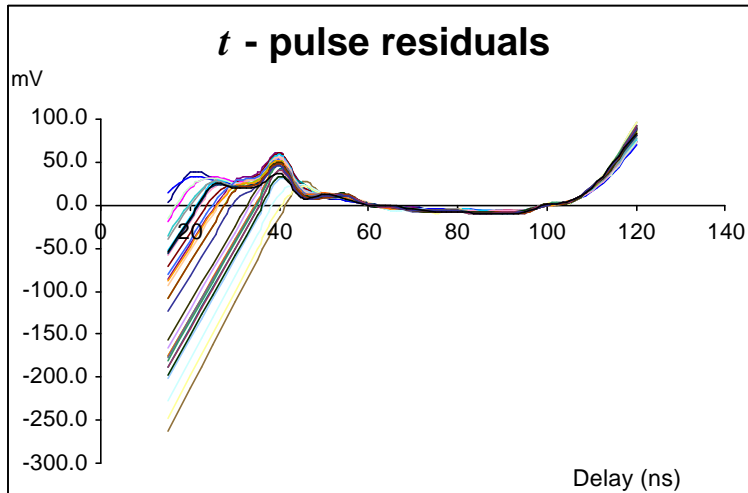


Figure 15. Residuals of  $t$ -pulse measurements after linear fit.

A minimum amplitude of pulse is necessary to get reliable  $t$ -pulse data. As shown in Figure 16, somewhere around a 30 to 40 fC injected pulse is needed to keep the amplitude of the  $t$ -pulse independent of the amount of injected charge. Over that level,  $\partial t/\partial A$  is about 0.55%, corresponding to shifts in the  $t$ -pulse corresponding to less than 1 ns. Relative to pulse amplitude,  $\partial t/\partial Q$  is about 55  $\mu\text{V}/\text{fC}$ ; the time shift appears to flatten out when the input pulse saturates the amplifier. Below that level, not only does the central value of the reported pulse time drift, there is a larger scatter in the amplitude of the  $t$ -pulses. Figure 17 is a plot of the dispersion in the  $t$ -pulse for small injected charges. It is derived by

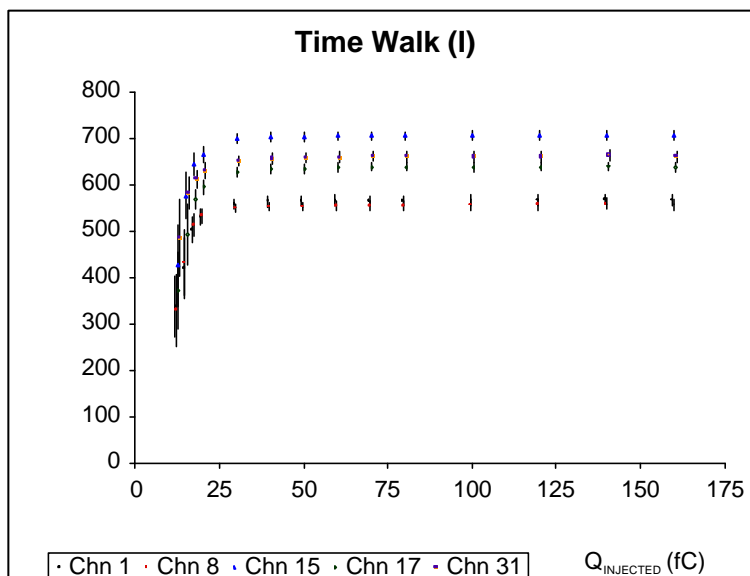


Figure 16. Variation in  $t$ -pulse measurements with changing injected pulse amplitudes.

taking the peak-to-peak spread of traces stored on an oscilloscope and dividing by three. This peak-to-peak reading technique was benchmarked against a set of 100 independent traces and found to actually return a  $3\sigma$  spread of a Gaussian noise distribution to the  $\sim 10\%$  level. The dispersion in the region plotted in Figure 17 is approximately  $1290 \exp(-Q_{\text{INJ}}/\pi)$ , but extrapolation to lower charge levels is hazardous.

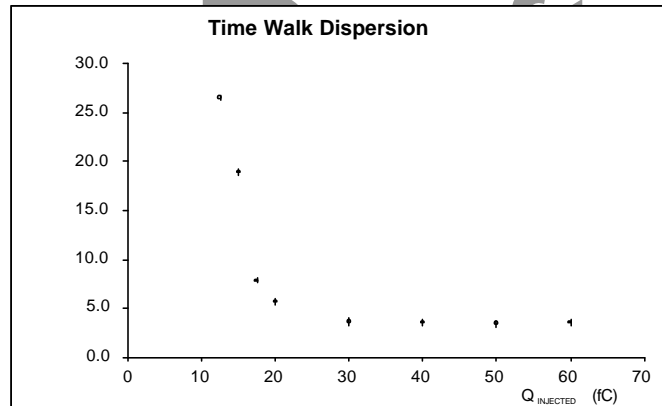


Figure 17. Approximate  $1\sigma$  spread in  $t$ -pulse amplitudes as function of injected test pulse charge.

### Conclusion

The TRIP-t prototype has been bench tested. Operating parameters and input timing diagrams have been developed that are expected to be close to the final operating conditions. The performance has been characterized with these conditions. Except for an evidently easily fixed problem with the output driver stage that follows the analog pipeline, the performance is good. Reliable  $t$ -pulse information, which will be of great use in the reconstruction, will be available for pulse that are about 4 to 5 photoelectrons over threshold<sup>3</sup>.

<sup>3</sup> A minimally ionizing particle at zero rapidity is produces a mean of about 8 photoelectrons in each fiber.